ACS OMEGA

http://pubs.acs.org/journal/acsodf

Article

Efficient Entrapment of Carbonic Anhydrase in Alginate Hydrogels Using Liposomes for Continuous-Flow Catalytic Reactions

Junshi Moriyama and Makoto Yoshimoto*

Cite This: *ACS Omega* 2021, 6, 6368−6378

Read Online

ACCESS | Metrics & More | Article Recommendations | Supporting Information

ABSTRACT: A versatile approach to entrap relatively small enzymes in hydrogels allows their diverse biotechnological applications. In the present work, bovine carbonic anhydrase (BCA) was efficiently entrapped in calcium alginate beads with the help of liposomes. A mixture of sodium alginate (3 wt %) and carbonic anhydrase−liposome conjugates (BCALs) was dripped into a Tris-HCl buffer solution (pH = 7.5) containing 0.4 M $CaCl_2$ to induce the gelation and curing of the dispersed alginate-rich droplets. The entrapment efficiency of BCALs, which was defined as the amount of catalysts entrapped in alginate beads relative to that initially charged, was 98.7 ± 0.2% as determined through quantifying BCALs in the filtrate being separated from the beads. When free BCA was employed, on the other hand, a significantly lower entrapment efficiency of 27.2 ± 4.1% was obtained because free BCA could pass through alginate matrices. Because the volume of a cured alginate bead (10 μL) entrapped with BCALs was about 2.5 times smaller than that of an original droplet, BCALs were densely present in the beads to give the concentrations of lipids and BCA of 4.6−8.3 mM and 1.1−1.8 mg/mL, respectively. Alginate beads entrapped with BCALs were used to catalyze the hydrolysis of 1.0 mM *p*-nitrophenyl acetate (*p*-NA) at pH = 7.5 using the wells of a microplate or 10 mL glass beakers as batch reactors. Furthermore, the beads were confined in a column for continuous-flow hydrolysis of 1.0 mM *p*-NA for 1 h at a mean residence time of 8.5 or 4.3 min. The results obtained demonstrate that the conjugation of BCA to liposomes gave an opportunity to achieve efficient and stable entrapment of BCA in alginate hydrogels for applying to catalytic reactions in bioreactors.

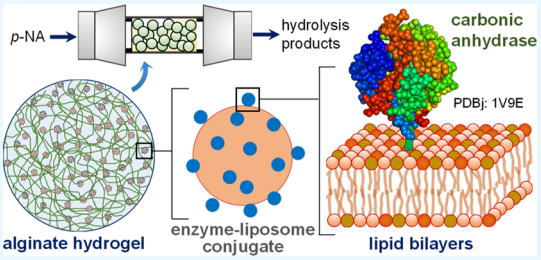

INTRODUCTION

Alginates are linear copolymers that consist of β-D-mannuronic acid and α-L-guluronic acid. Gelation of anionic alginates occurs in an aqueous solution in the presence of multivalent cations like calcium ions, which can predominantly cross-link polyguluronate sequences among multiple polymer chains.[1] Hydrogels of calcium alginate were utilized to prepare biologically active immobilized enzymes and cells,[2−6] and biomedical materials.[7,8] Alginate bead-entrapped enzymes are applicable to various catalytic bioprocesses and biomaterials.[9−11] One of the critical requirements for hydrogel beads entrapped with enzymes is that the enzyme molecules are retained stably in polymeric matrices during storage and under various reaction conditions. The mechanical and physicochemical properties of alginate-based materials are dependent strongly on the chemical structure and concentration of alginates,[12] and the type of divalent cations used for gelation.[13,14] Concerning the porosity of alginate matrices, there can be a trade-off relationship between the prevention of enzyme leaching from the hydrogels and keeping sufficient mass transfer characteristics with respect to substrates and products within the matrices. In this regard, several different approaches were reported to control the leaching of enzymes from alginate beads. One of the approaches is surface coating of alginate beads with charged polymers.[3,15,16] However, this can result in an increased mass transfer resistance at the interface between the bulk solution and gel phase. On the other hand, cross-linked aggregates of enzymes were entrapped in alginate beads.[9,11,17,18] Alginate hydrogels possess pores with a wide size distribution.[12] Therefore, cross-linking of enzymes prior to entrapment in alginate beads can give an opportunity to facilitate enzyme retention in the beads. A potential drawback of this approach is that the preparation of enzyme aggregates needs to be carried out under the optimized conditions that the enzyme molecules of interest are sufficiently cross-linked without causing significant negative effects on the enzyme structure and substrate accessibility.

Alginate beads entrapped with liposomes were reported, in which the liposomes encapsulated with small molecular mass compounds such as drugs and fluorescent dye were employed.[19,20] Liposomes are attractive particles to be entrapped in hydrogels in the sense that soft colloidal nature of liposomes allows to control their size and that physicochemical characteristics of liposomes can be tuned on

Received: December 27, 2020
Accepted: February 10, 2021
Published: February 22, 2021

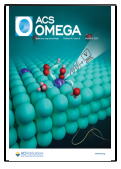

https://dx.doi.org/10.1021/acsomega.0c06299
ACS Omega 2021, 6, 6368−6378

the basis of chemical structures of lipids used. Moreover, synthetic polymers and biopolymers including enzymes can be covalently conjugated to the surface of liposomes.[21−23] We reported that the bovine carbonic anhydrase (BCA) molecules could be densely conjugated to the surface of carboxyl group-bearing liposomes.[23] Enzyme−liposome conjugates, which possess a much larger size than single-enzyme molecules, may potentially be applicable to stable entrapment of enzymes in alginate beads even without their surface coating. There have been a limited number of literature reports associated with the entrapment of enzyme−liposome conjugates in hydrogel beads. Itel et al.[24] reported that alkaline phosphatase-loaded negatively charged liposomes could be entrapped in alginate-based microbeads, in which the enzyme-loaded liposomes were applied as a model of matrix vesicles. The role of liposomes in the entrapment process of enzymes in alginate beads has not been clarified so far.

In the work presented here, carbonic anhydrase−liposome conjugates (BCALs) were prepared and entrapped in hydrogel beads of calcium alginate, and the effect of liposomes on the entrapment efficiency of the enzyme was examined in detail through the comparison with the characteristics of the alginate beads entrapped with free BCA. Such a comparison as above contributes to clarify the characteristics of liposome-conjugated enzymes and assess the potential versatility of the present approach in entrapping other enzymes with relatively small molecular mass in hydrogels. In the previous literature, BCA was entrapped in alginate-based beads coated with chitosan.[15] Carbonic anhydrase and its immobilized forms are potentially applicable to various biotechnological processes including sequestration of carbon dioxide.[25−28] In this work, application of alginate beads entrapped with BCALs to the continuous-flow catalytic reaction was demonstrated.

EXPERIMENTAL SECTION

Materials. Carbonic anhydrase from bovine erythrocytes (BCA, EC 4.2.1.1) (catalog number, C2624, lot SLBL1750V, lot SLBX5393) was obtained from Sigma-Aldrich. The molar absorption coefficient of BCA of ε_{280} = 56,000 $M^{-1}\cdot cm^{-1}$ was taken.[29] Sodium alginate (catalog number 194-13321, lot KWQ3038), calcium chloride dihydrate ($CaCl_2\cdot 2H_2O$) (lot SAF5613), boric acid (lot SDQ6029), and acetonitrile (DSN3682) were obtained from Wako Pure Chemical Industries (Osaka, Japan). 4-Nitrophenyl acetate (*p*-NA) (lot XYIRO-RE) was obtained from TCI (Tokyo, Japan). 1-Palmitoyl-2-oleoyl-*sn*-glycero-3-phosphocholine (POPC) (commercial name: COATSOME MC-6081, lot 16096811FL), 1-palmitoyl-2-oleoyl-*sn*-glycero-3-phosphoglycerol, sodium salt (POPG-Na) (COATSOME MG-6081LS, lot 15066951L, lot 14066951L), and 1-palmitoyl-2-oleoyl-*sn*-glycero-3-phosphoethanolamine-*N*-(glutaryl) (COATSOME FE-6081GL, NG-POPE) (lot 10016961A5) were obtained from NOF (Tokyo, Japan). 1-Ethyl-3(3-dimethylaminopropyl)carbodiimide (lot DQ143) and 2-morpholinoethanesulfonic acid, monohydrate (MES) (lot NT015) were obtained from Dojindo Laboratories (Kumamoto, Japan). *N*-Hydroxysulfosuccinimide sodium salt (sulfo-NHS) (lot BCBQ8798V) and 5(6)-carboxyfluorescein (CF) (lot BCBQ7825V) were obtained from Sigma-Aldrich. 2-Amino-2-hydroxymethyl-1,3-propanediol (Tris) (lot LKN5666) was obtained from FUJIFILM Wako (Osaka, Japan). All chemicals were used as received. Water was treated with a water purification system Elix UV3 Essential from Merck.

Buffer Solutions Used. Buffer solutions prepared and used in this work were abbreviated as follows. TB1: 50 mM Tris-HCl buffer solution (pH = 9.0), TB2: 50 mM Tris-HCl buffer solution (pH = 7.5), and MESB: 5.0 mM MES buffer solution (pH = 5.5).

Preparation of BCALs. The BCA molecules were covalently conjugated to the carboxyl group-bearing liposomes composed of POPC, POPG, and NG-POPE (65:20:15 in mole ratio) according to the method reported previously.[23] For details, see Figure S1 in the Supporting Information. In this work, BCALs possessing different numbers of enzyme molecules per liposome and different hydrodynamic diameter, D_h, were prepared for their entrapment in alginate beads. Purified BCALs suspended in TB1 were stored in the dark at 4 °C in a 1.5 mL polypropylene tube until use.

Measurements of Enzyme Activity of BCALs and Free BCA. The esterase activity of BCALs or free BCA was determined in TB2 with 1.0 mM *p*-NA as the substrate. To initiate the reaction, a stock solution of *p*-NA (100 mM, 15 μL) in acetonitrile was mixed with TB2 containing enzyme to give a total volume of 1.5 mL and the initial concentration of *p*-NA of 1.0 mM (1 vol % acetonitrile in a reaction mixture). Note that the stock suspension of BCALs was diluted 30 times in the assay mixture. Therefore, the difference in the pH values between the stock suspension of BCALs in TB1 (pH = 9.0) and the assay mixture in TB2 (pH = 7.5) was assumed to be negligible. Measurements were performed at 25 °C in a quartz cuvette with an optical path length of l = 1.0 cm. The absorbance at 405 nm (A_{405}) was followed as a measure of the formation of *p*-nitrophenolate being one of the hydrolysis products for 3 min using a spectrophotometer V-550 from JASCO (Tokyo, Japan) equipped with a Peltier-type temperature controller (EHC-477S). The concentration of *p*-nitrophenolate was calculated with a molar absorption coefficient ε_{405} of 10,510 $M^{-1}\cdot cm^{-1}$.[30] The rate of the formation of *p*-nitrophenolate was determined on the basis of the slope obtained by plotting A_{405} versus time. Because the background reaction is not negligible, the rate obtained with TB2 alone was subtracted from the rate with BCALs or free BCA.

Entrapment of BCALs or Free BCA in Calcium Alginate Beads. The concentrations of sodium alginate and $CaCl_2$ used in the preparation of alginate beads were optimized on the basis of a series of preliminary experiments, see Figure S2. Sodium alginate powder (15 mg) was mixed with a BCAL suspension in TB1 (0.5 mL) in a 1.5 mL polypropylene tube to give the concentration of sodium alginate of 3 wt %. The above mixture was incubated at room temperature for 3−24 h to induce complete solubilization of sodium alginate. Then, aliquots (25 μL) of the above viscous mixture were dripped into TB2 (10 mL) containing 0.4 M $CaCl_2$ being stirred in a 20 mL glass beaker. To define the volume of each droplet as precisely as possible, a pipet (Microman M25) with a capillary piston from Gilson was used for the manual dripping process. With the above procedure, noncoalescent and almost spherical beads were formed in the $CaCl_2$-containing TB2 because calcium ions caused rapid gelation of the negatively charged alginate at the surface of droplets. The bead suspension was continuously stirred for 2 h at room temperature (≈25 °C) using a magnetic stirrer to induce the diffusion of calcium ions into the droplets for their further gelation and curing. The beads were recovered by the filtration with a filter paper no. 2

https://dx.doi.org/10.1021/acsomega.0c06299
ACS Omega 2021, 6, 6368−6378

(110 mm in diameter) (lot 40210057) from Toyo Roshi Kaisha (Tokyo, Japan) and stored in TB2 at 4 °C until use. The filtrate was analyzed to determine the amount of BCALs unentrapped (see below). The alginate beads entrapped with free BCA were also prepared as described above except that sodium alginate was solubilized with TB1 containing free BCA. The concentration of free BCA in the sodium alginate solution was adjusted so that the esterase activity with 1.0 mM *p*-NA as the substrate (see above) was the same as that of the corresponding sodium alginate solution containing BCALs. For this, the separately determined relationship between the esterase activity and concentration of free BCA in TB2 was used, see Figure S3. The beads consisting of alginate alone (denoted as "empty" beads) were prepared under the same conditions as described above except that sodium alginate (3 wt %) was solubilized with enzyme-free TB1. The diameter of above alginate beads was measured by analyzing the images of each bead being taken by using the fluorescence microscope instrument BZ-X810 from KEYENCE (Osaka, Japan).

Determination of the Entrapment Efficiency *E* of BCALs or Free BCA in Alginate Beads. The entrapment efficiency, E_{BCAL}, for BCALs or E_{Free} for free BCA in alginate beads was determined as follows. The filtrate, which was obtained by filtrating the beads suspended in the $CaCl_2$-containing TB2 after the gelation step, was analyzed in terms of its intrinsic fluorescence spectrum. The fluorescence measurements were performed at 25 °C at an excitation wavelength of 295 nm using a spectrofluorometer FP-8200 from JASCO equipped with a Peltier-type temperature controller (ETC-814). The emission fluorescence intensity was recorded at wavelengths λ ranging from 300 to 550 nm. Then, the fluorescence intensity I_f at λ = 343 nm was obtained. The intensity, I_{100} at λ = 343 nm, which corresponds to the intensity that all of the BCALs or free BCA molecules charged are present in a filtrate (100% leaching), was also measured. For this, a BCAL suspension or a free BCA solution, which was the same in each concentration of enzyme as the concentration employed in the solubilization of sodium alginate for preparing alginate beads, was diluted 20 times with the filtrate obtained in the preparation of empty beads. The above "20 times dilution" is consistent with the volume ratio of a sodium alginate solution (0.5 mL) to the bulk solution (10 mL) employed in the preparation of the beads (see above). The entrapment efficiency, E_{BCAL} or E_{Free}, was calculated as $E = (I_{100} - I_f)/(I_{100} - I_C)$, where I_C is the fluorescence intensity at λ = 343 nm with respect to the filtrate obtained in the preparation of empty beads. The measurements of the UV/vis absorbance spectra were also performed with respect to the samples to which the above fluorescence measurements were performed.

Entrapment of 5(6)-Carboxyfluorescein-Containing Liposomes in Alginate Beads. The leakage of CF from liposomes during their entrapment in alginate beads was examined to evaluate the integrity of liposome membranes in alginate matrices. The CF molecules were encapsulated in liposomes composed of POPC, POPG, and NG-POPE (mole ratio 65:20:15) with MESB, see Figure S4. The bulk solution (MESB) suspending 5(6)-carboxyfluorescein-containing liposomes (CFLs) was replaced with TB1 by passing the CFLs through the gel permeation chromatography column using TB1 as the eluent. CFLs were entrapped in alginate beads under the same conditions as described above except that sodium alginate was solubilized with a CFL suspension (0.5 mL) at a total lipid concentration of 9.5 mM. The filtrate (≈10 mL) obtained by separating cured beads was recovered for fluorescence measurements. If all of CFLs charged were present in the filtrate being corresponding to the case of 100% leaching, the concentration of lipids in the filtrate can be calculated as 0.48 mM. The filtrate was diluted 480 times and its fluorescence spectrum was measured at an excitation wavelength of 490 nm using the spectrofluorometer. The above procedure allows to directly compare the spectrum of the filtrate with the spectrum separately measured with respect to a TB2 solution suspending CFLs at [lipids] = 1.0 μM in order to estimate the fractional leakage of CF from the entrapped liposomes. The fluorescent measurement was also performed with respect to a mixture of a CFL suspension (1.0 mL, [lipids] = 1.0 μM) and 400 mM sodium cholate solution (110 μL) for the solubilization of lipid membranes. All measurements were performed at 25 °C. Note that the above experiments were performed with CFLs without being conjugated with enzyme.

Batch Reactions Catalyzed by Single Alginate Beads Entrapped with BCALs. *Catalytic Hydrolysis of p-NA.* The esterase activity of single beads entrapped with BCALs was measured using the microplate wells as reaction vessels. Each bead was bathed in TB2 (198 μL) and the beads were moved at one side of the bottom of each well by tilting the microplate. Then, 2.0 μL of an acetonitrile solution containing 100 mM *p*-NA was added to each well using a Pipetman L multichannel (model P8x200L) from Gilson to initiate the reaction. The microplate was set into a spectrophotometer instrument Epoch from BioTek (Vermont, U.S.A.). The absorption of the reaction mixtures without being stirred was measured. The absorbance at 405 nm (A_{405}) was continuously recorded for 10 min. All reactions were performed at room temperature (≈25 °C). The reactions catalyzed by (unentrapped) BCALs were also performed under the same overall concentration of enzyme as the case of the reactions catalyzed by the entrapped BCALs. The total volume of the BCAL-catalyzed reactions was 214 μL. Furthermore, the A_{405} value of TB2 initially containing 1.0 mM *p*-NA was followed for 10 min in the presence of single empty beads. In separate experiments, batch reactions were performed with multiple alginate beads as follows. The alginate beads entrapped with BCALs or free BCA were suspended in TB2 to give a total volume of 10 mL in a 10 mL glass beaker. The suspension was stirred with a magnetic stirrer at room temperature (≈25 °C). An acetonitrile solution (101 μL) containing 100 mM *p*-NA was added to the suspension to initiate the hydrolysis reaction. At a reaction time of 10 min, an aliquot (1.5 mL) was withdrawn and the A_{405} value was measured at 25 °C. The beads were recovered by the filtration and TB2 (10 mL) was added followed by being incubated for 20 min without stirring. The washed beads were then recovered by filtration. This procedure was repeated twice. The above reaction cycle was performed for eight times to evaluate reusability of the beads. The background hydrolysis of *p*-NA was measured in a quartz cuvette at 25 °C.

Catalytic Hydration of Carbon Dioxide. The enzymatic hydration of carbon dioxide and the formation of calcium carbonate particles were examined as follows using the wells of a microplate as reaction vessels. In each well, a Tris solution (1.39 M, 43.3 μL) was mixed with water (46 μL) containing 200 mM $CaCl_2$, followed by the addition of a bead entrapped with BCALs or free BCA, or an empty bead. Then, carbon dioxide-saturated water (110.7 μL) being prepared by

https://dx.doi.org/10.1021/acsomega.0c06299
ACS Omega 2021, 6, 6368−6378

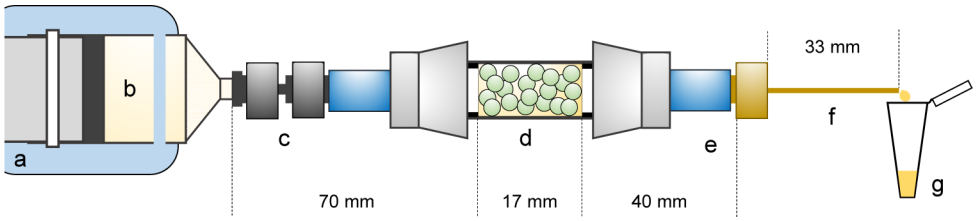

Figure 1. Schematic illustration of the continuous-flow catalytic reactor used. (a) Syringe pump, (b) syringe containing substrate solution (1.0 mM *p*-NA), (c) connectors made of PEEK, and (d) reactor column made of borosilicate glass. Alginate beads entrapped with BCALs or free BCA, or empty beads were confined in the column, (e) connector made of PEEK, (f) outlet tube made of PEEK, and (g) polypropylene microtube with a 1.5 mL volume for collecting samples containing reaction products.

introducing carbon dioxide gas into an external loop airlift bubble column[23] was added to the above well. The turbidity of the bulk solution was followed at the absorption at 600 nm as a measure of the formation and accumulation of calcium carbonate for 10 min at about 17 °C without mechanical mixing. The above measurements were also performed with the carbon dioxide-containing water, which was prepared by diluting the above saturated solution two times.

Continuous-Flow Catalytic Reactions with Alginate Beads Entrapped with BCALs. The flow reactor used is schematically illustrated in Figure 1. Alginate beads entrapped with BCALs or free BCA were confined in a glass chromatography column Omnifit (OME6710, 6.6 mm (i.d.) × 17 mm in length, and total volume 0.58 mL) from Diba Industries (Mahopac, NY, U.S.A.). To remove air bubbles in the reactor, the column was placed vertically and a TB2 solution (about 1 mL) was passed slowly through the reactor. The inlet made of polyetheretherketone (PEEK) was connected to a 10 mL polypropylene syringe SS-10SZ from Terumo (Tokyo, Japan) filled with TB2 containing 1.0 mM *p*-NA and 1 vol % of acetonitrile. Then, the *p*-NA-containing TB2 was passed through the column confined with the beads at a flow rate of 68 or 137 μL/min using a syringe pump instrument YSP-201 from YMC (Kyoto, Japan). The reaction solutions were pooled every 1 min in 1.5 mL polypropylene tubes at the reactor outlet. Then, an aliquot (5.0 μL) was withdrawn from the pooled fraction and analyzed in terms of the absorbance at 405 nm with a spectrophotometer V-630 Bio from JASCO equipped with a cell holder SAH-769 One Drop for microvolume measurements. The optical path length was l = 0.1 cm. The measurements were performed immediately after collecting each fraction. The above reaction operation was also performed with empty alginate beads. All of the reaction operations and measurements were performed at room temperature (≈25 °C).

RESULTS AND DISCUSSION

Entrapment Efficiency of BCALs or Free BCA in Alginate Beads. BCALs were prepared and purified as we reported previously,[23] see Figure S1. In the present work, BCALs, which were different in the apparent number of biologically active enzyme molecules per liposome and in the mean hydrodynamic diameter, D_h, were prepared as shown in Table 1. A suspension of BCALs (25 μL) containing 3 wt % sodium alginate was dripped using a micropipet into a stirred 0.4 M $CaCl_2$-containing TB2 followed by being incubated for 2 h to induce the formation of cured alginate beads. The average diameter of the beads entrapped with BCALs was 2.7 ± 0.2 mm, as determined with respect to a batch of preparation on the basis of the microscope analyses. The photograph of the beads is shown in Figure S5A. Accordingly, the average volume of a bead was calculated as 10 μL being about 2.5 times smaller than the original volume of a sodium alginate droplet used for gelation (25 μL).

Table 1. Entrapment of BCALs in Calcium Alginate Beads

	no. 1	no. 2	no. 3	no. 4
mean hydrodynamic diameter of BCALs, D_h/nm	86	156	82	138
ζ-potential of BCALs/mV	−44.0	−29.6	−27.0	−28.6
number of biologically active BCA per liposome	513	1259	440	1369
apparent concentration of biologically active BCA in sodium alginate solution/μM	14.7	15.1	25.0	17.2
total concentration of lipids in sodium alginate solution/mM	1.85	2.64	3.33	2.16
entrapment efficiency E_{BCAL}/%	99.0	98.6	98.7	n.d.[a]

[a]For the fluorescence spectrum of the filtrate being separated from the alginate beads entrapped with BCALs, see Figure S6C-1. The spectrum shows negligible fluorescence intensity, meaning that the E_{BCAL} value with respect to no. 4 is comparable to the values of other preparations, although we could not measure the spectrum corresponding to 100% leaching for the calculation of the E_{BCAL} value because of the shortage of the corresponding BCAL sample.

To determine the entrapment efficiency of BCALs on the basis of the amount of enzyme, E_{BCAL}, the filtrate, which was obtained by filtrating a $CaCl_2$-containing TB2 suspending the beads entrapped with BCALs, was analyzed in terms of the intrinsic fluorescence and UV/vis absorption spectra. The results of fluorescence measurements are shown in Figure 2. The BCALs used in the figure correspond to no. 2 in Table 1. Practically no emission intensity peak is seen with respect to the filtrate separated from the beads (curve 1 in Figure 2A). On the other hand, the BCAL suspension, which was separately prepared to estimate the spectrum equivalent to 100% leaching of BCALs, exhibits a large emission intensity peak at λ = 343 nm (curve 2). Accordingly, the E_{BCAL} value could be calculated as 98.7%. The average values of E_{BCAL}, which was obtained with three independent preparations of the beads, was 98.7 ± 0.2% (mean value ± standard deviation). These results clearly demonstrate that almost all of the initially charged BCALs were efficiently entrapped in alginate beads. In other words, practically no leaching of BCALs occurred even at the early stage of the gelation process of alginates. Furthermore, this result also demonstrates that BCALs remained inside the beads during their curing, which caused squeezing water from the beads into bulk solution. Because the volume of a cured bead (10 μL, see above) is about 2.5 times smaller than the initial volume of a droplet of a sodium alginate/BCALs mixture (25 μL, [lipid] = 2.64 mM,

https://dx.doi.org/10.1021/acsomega.0c06299
ACS Omega 2021, 6, 6368−6378

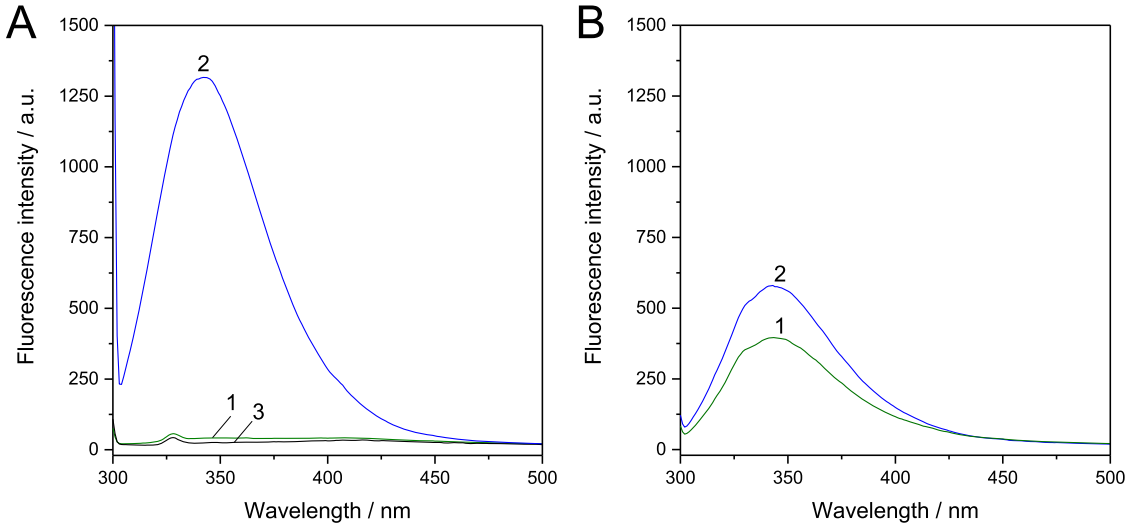

Figure 2. (A) Curve 1 shows the intrinsic fluorescence spectrum of the filtrate obtained by filtrating the $CaCl_2$-containing TB2 used to induce the formation of alginate beads entrapped with BCALs. Curve 2 shows the spectrum obtained with respect to the BCAL suspension being diluted with TB2 to give the concentrations of biologically active BCA and total lipids of 0.76 μM and 0.13 mM, respectively. The dilution was carried out with the $CaCl_2$-containing TB2 being the filtrate in the preparation of empty beads so that the concentrations of calcium ion in the above measurements (curves 1 and 2) are comparable. This BCAL suspension (curve 2) is regarded as the hypothetical filtrate in which all of the BCALs charged are present, being the case corresponding to 100% leaching of BCALs, if occurred, from alginate beads. Curve 3 shows the spectrum of filtrate obtained by filtrating empty beads. Above data correspond to no. 2 in Table 1. (B) Curves 1 and 2 were obtained under the same conditions as described above with respect to the curves 1 and 2 in the panel A, respectively, except that free BCA was used in the panel B instead of BCALs. The apparent amount of biologically active BCA charged ([BCA] = 15.1 μM) was the same between the preparations of alginate beads entrapped with BCALs and free BCA, see no. 2 in Table 2. Because BCA is partially inactive on the surface of liposomes,[23] the total amount of enzyme in the BCAL suspension charged is larger than that in the free BCA solution. The maximum fluorescence intensity of the former suspension (curve 2 in panel A) is, therefore, larger than that of latter solution (curve 2 in panel B). For the control spectrum, see curve 3 in the panel A. All measurements were performed at 25 °C at an excitation wavelength of 295 nm.

$[BCA]_{active}$ = 15.1 μM, see the no. 2 in Table 1), the concentrations of lipids and BCA in the cured beads can be estimated as 6.60 mM and 37.8 μM (1.1 mg/mL), respectively. The same analysis was applied with respect to the entrapment of free BCA in alginate beads, see Figure S5B for the photograph of the beads prepared. For the filtrate being separated from the beads entrapped with free BCA corresponding to no. 2 in Table 2, the peak of fluorescence emission intensity is clearly seen (curve 1 in Figure 2B), meaning that unentrapped free BCA molecules were present in bulk solution (filtrate). With the peak intensity obtained with respect to the free BCA solution corresponding to 100% leaching (curve 2 in Figure 2B), the entrapment efficiency E_{Free} could be calculated as 33.2%. The mean E_{Free} value obtained with four independent preparations of the beads was 27.2 ± 4.1%. This means that significant leaching of the free BCA molecules from alginate droplets occurred during their gelation and curing processes.

Table 2. Entrapment of Free BCA in Calcium Alginate Beads

	no. 1	no. 2	no. 3	no. 4
concentration of free BCA in sodium alginate solution/μM	14.7	15.1	25.0	17.2
entrapment efficiency E_{free}/%	26.1	33.2	24.0	25.4

We also performed the UV/vis absorption measurements with respect to the filtrates obtained in the preparation of alginate beads entrapped with BCALs or free BCA (Figure 3). A similar trend is seen between the UV/vis absorption (Figure 3) and fluorescence (Figure 2) spectra. Practically no absorption peak is seen for the filtrate being separated from the beads entrapped with BCALs (curve 1 in Figure 3A). On the other hand, the absorption spectrum of BCALs corresponding to 100% leaching (curve 2) shows both the turbidity derived from colloidal liposomes and the specific absorbance peak at 280 nm derived from the liposome-conjugated BCA. Therefore, almost all BCALs charged were confirmed to be entrapped in alginate beads. Although the concentration of $CaCl_2$ in alginate droplets is unknown, BCALs may have an opportunity to form clusters within the droplets in the presence of calcium ions.[31] As for the entrapment of free BCA, a clear absorption peak is seen for the filtrate being separated from the beads (curve 1 in Figure 3B). The relative value of absorption of the filtrate at 280 nm to the free BCA solution corresponding to 100% leaching (curve 2 in Figure 3B) is comparable to that observed with the fluorescence measurements (Figure 2B), confirming the low entrapment efficiency of free BCA. For different preparations of alginate beads entrapped with BCALs or free BCA, the results are consistent, see Figure S6.

Plausible reasons for the observed high entrapment efficiency of BCALs in alginate beads are as follows. (i) Colloidal liposomes (D_h = 82−156 nm) are advantageous to promote the retention of liposome-conjugated enzyme molecules in the matrices of alginate, whereas the free BCA molecules (≈4.1 nm in hydrodynamic diameter[32]) can pass through the matrices resulting in significant leaching into bulk solution. (ii) Calcium ion-induced partial clustering of BCALs potentially occurred in alginate phase during the gelation and curing processes. The curing process causes a significant shrinkage of the beads. Therefore, the concentration of BCALs

https://dx.doi.org/10.1021/acsomega.0c06299
ACS Omega 2021, 6, 6368−6378

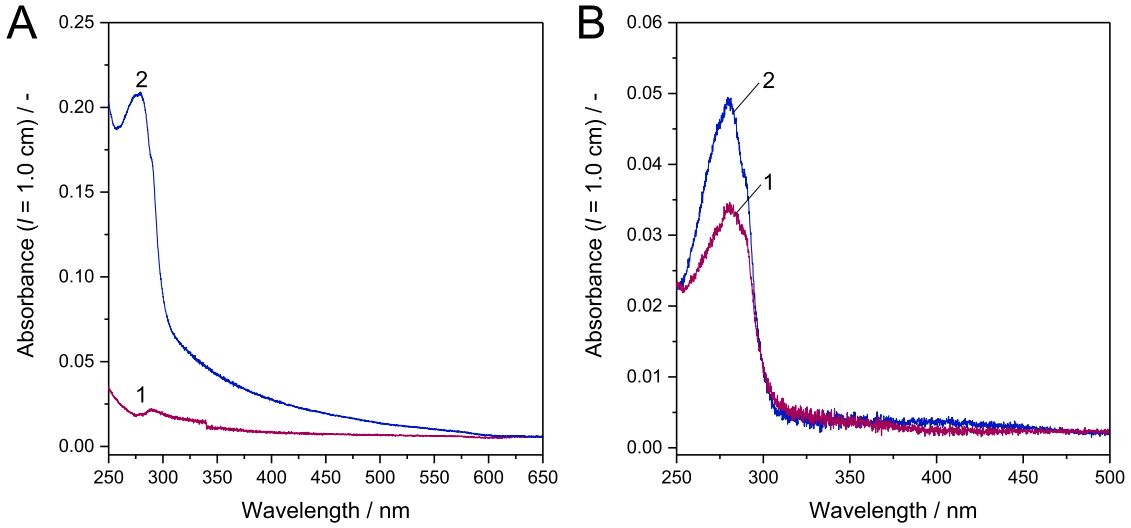

Figure 3. (A) Curve 1 shows the UV/vis absorption spectrum of filtrate obtained in the preparation of alginate beads entrapped with BCALs. Curve 2 shows the spectrum of the BCAL suspension prepared with the $CaCl_2$-containing TB2 being the filtrate obtained in the preparation of empty beads. The concentration of BCALs ($[BCA]_{active}$ = 0.76 μM, [lipid] = 0.13 mM) in the suspension corresponds to that at 100% leaching of BCALs from the beads. Each absorption spectrum is shown against the TB2 containing $CaCl_2$ obtained in the preparation of the empty beads. (B) Curves 1 and 2 were obtained under the same conditions as curves 1 and 2 in the panel A, respectively, except that free BCA was used in the panel B instead of BCALs. All measurements were performed at 25 °C. Note that scales of abscissa and ordinate are different between the panels A and B.

in the alginate phase increases, which can be a factor facilitating the calcium ion-induced clustering of BCALs. The above event should also be advantageous to keep the BCALs stably within the polymeric matrices being large enough to pass through the free BCA molecules. The conformational state of enzymes may be affected by the interaction with calcium alginate. Although the structural characteristics of enzymes entrapped in alginate beads are difficult to be clarified, in the present work, the activity of bead-entrapped enzymes was examined on the basis of batch or continuous-flow reactions with *p*-NA as the substrate in which mass transfer effects are also involved. Based on the results obtained so far, the alginate bead entrapped with BCALs is schematically illustrated in Figure 4 with the photograph of the bead.

Physical Stability of Liposome Membranes in Alginate Beads. CFLs composed of POPC, POPG, and POPE-NG (mole ratio: 65:20:15) were entrapped in alginate beads and the integrity of lipid membranes in the beads was examined on the basis of leakage of the liposome-encapsulated fluorescent dye molecules. For this, the liposomes without being conjugated to enzyme were employed. Curves 1 and 2 in Figure 5 show the spectra corresponding to the hypothetical cases of 100% CF leakage from entrapped liposomes (all CF molecules are present in the bulk solution and the alginate phase at the same concentration) and no entrapment of CFLs

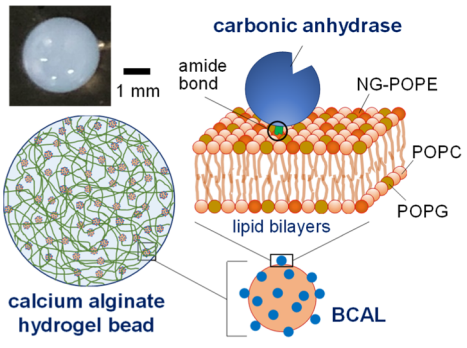

Figure 4. Photograph of an alginate hydrogel bead entrapped with BCALs, and schematic illustrations of an alginate bead entrapped with BCALs and phospholipid bilayer membranes covalently conjugated with a carbonic anhydrase molecule.

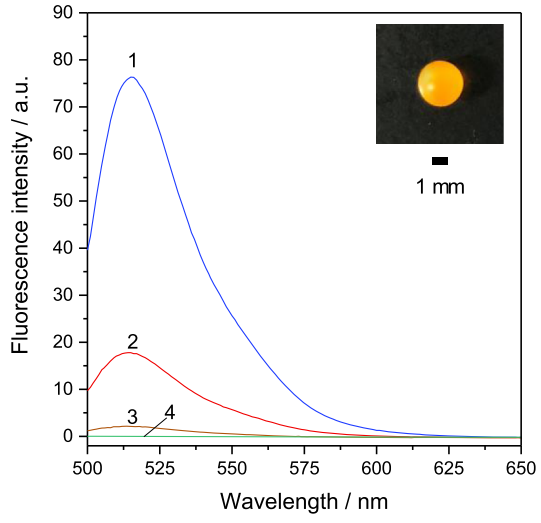

Figure 5. Curve 1 represents the fluorescence spectrum of CF in TB2 containing CFLs ([lipids] = 1.0 μM) in the presence of 40 mM sodium cholate for the solubilization of lipid membranes. Curve 2 represents the spectrum of TB2 suspending CFLs ([lipids] = 1.0 μM). Curve 3 represents the spectrum of diluted filtrate being recovered in the preparation of alginate beads entrapped with CFLs. The dilution of the filtrate was carried out so that the degree of leakage of CF from the entrapped CFLs can be evaluated by the direct comparison among the curves 1 (100% leakage of CF), 2 (all CFLs in the bulk solution), and 3 (filtrate) (see Experimental Section). Curve 4 represents the spectrum of TB2 alone. All measurements were performed at 25 °C at an excitation wavelength of 490 nm. The inset shows a photograph of an alginate bead entrapped with CFLs. A scale bar in the inset represents 1 mm.

https://dx.doi.org/10.1021/acsomega.0c06299
ACS Omega 2021, 6, 6368−6378

(all CFLs are unentrapped and thus present in the bulk solution), respectively. The filtrate in the preparation of alginate beads entrapped with CFLs was recovered for the fluorescence measurements. The curve 3 in Figure 5 represents the spectrum obtained with respect to the filtrate being diluted so that direct comparison is possible among the curves 1, 2, and 3 (see Experimental Section). The fluorescence intensity of the curve 3 is clearly smaller than the intensities of curves 1 and 2. This result demonstrates that almost all CF molecules remained encapsulated in liposomes being entrapped in alginate beads. The photograph of an alginate bead entrapped with CFLs is shown in the inset of Figure 5. The beads are orange colored, clearly confirming that the CF molecules are quenched in liposomes. The integrity of lipid membranes is, therefore, found to be little affected by the interaction with calcium alginate.

Catalytic Performance of Alginate Beads Entrapped with BCALs in Batch Reactors. *Catalytic Hydrolysis of p-NA.* To examine the catalytic performance of alginate beads entrapped with BCALs, the enzymatic hydrolysis of *p*-nitrophenyl acetate (*p*-NA) was examined using the wells of microplate as reaction vessels (Figure 6A). The initial reaction mixture consisted of TB2 (200 μL) containing 1.0 mM *p*-NA and a single bead entrapped with BCALs. In each well, an alginate bead was placed so that the effect of the bead on the measurements could be minimized (Figure 6B). The measurements were performed with three wells in parallel each of which contained a bead. For comparison, the reaction was performed with TB2 containing (unentrapped) BCALs at the comparable overall concentration of the biologically active enzyme to the case of single bead-catalyzed reactions. The reaction was also performed with single empty beads, see Figure S5C for the photograph of the beads. The results obtained with respect to the catalytic batch reactions are shown in Figure 6C. The empty beads are catalytically almost inactive (curve 3 in Figure 6C). On the other hand, the alginate beads entrapped with BCALs exhibit catalytic activity toward *p*-NA (curve 1 in Figure 6), although the initial rate of reaction is smaller than the reaction with unentrapped BCALs (curve 2). These results indicate that the overall rate of reaction catalyzed by the bead-entrapped BCALs is controlled by the mass transfer process. This is partly because the size of beads is large. The beads entrapped with free BCA exhibited negligible catalytic activity toward *p*-NA, see Figure S7, suggesting that significant leaching of free BCA from the hydrogel phase to the bulk solution occurred during the storage of the beads. Multiple alginate beads entrapped with BCALs or free BCA were used for the repeated hydrolysis of *p*-NA in a 10 mL glass beaker as a batch reactor. Each reaction time was 10 min and the beads were recovered from the reaction mixture by filtration and incubated in TB2 for 20 min. The results obtained are shown in Figure S8. The concentrations of products being catalytically produced with alginate beads entrapped with BCALs showed 90−115 μM throughout the repeated use eight times. On the other hand, the alginate beads entrapped with free BCA gave 21 μM of catalytically produced products in the 1st reaction followed by a significant decrease in the catalytic activity in the second to eighth reactions. This indicates that leaching of free BCA molecules from the beads occurred in the first reaction cycle and the free BCA molecules in the bulk solution were removed by the filtration.

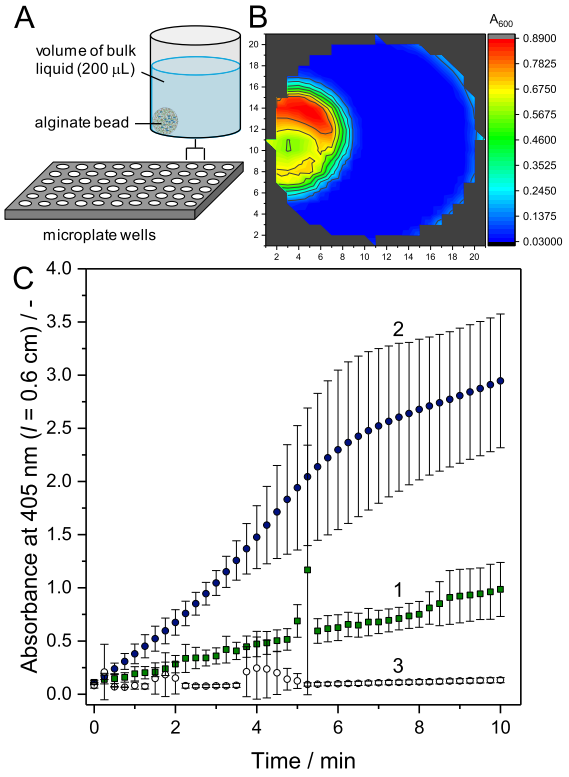

Figure 6. (A) Schematic illustration of a bath-mode reaction with a single alginate bead using the well of a microplate as a reaction vessel. (B) Area-scan analysis of a well in which an alginate bead was placed at the bottom of the vessel. The matrix size was 21 × 21 and the area-scan was performed at an absorbance wavelength of 600 nm. (C) Curve 1 (squares) shows the time course of the hydrolysis of *p*-NA catalyzed by single alginate beads entrapped with BCALs in the wells. The absorbance was measured at the center of the well and a single bead was placed in the well so that the absorbance measurement was little affected by the bead, see the panel B. Curve 2 (blue circles) shows the hydrolysis of *p*-NA catalyzed by (unentrapped) BCALs at a concentration of enzyme of 14.7 μM being comparable to the overall concentration employed in the single bead-catalyzed reactions. For the reactions, the BCALs no. 1 shown in Table 1 were used. Curve 3 (empty circles) shows the reaction with the single empty beads. All measurements were performed in TB2 with the microplate reader instrument.

Catalytic Hydration of Carbon Dioxide. The alginate beads entrapped with BCALs were applied to catalyze the hydration of CO_2 to facilitate the formation of calcium carbonate particles in the presence of calcium ions. A CO_2-saturated water (110.7 μL) was mixed with the Tris solution (89.3 μL) containing single beads entrapped with BCALs and 102 mM $CaCl_2$ using microplate wells as reaction vessels. The Tris solution was used to keep appropriate pH for the formation of calcium carbonate.[33] Three-parallel reactions were performed under each reaction condition. As a measure of the formation of particles, turbidity of the mixtures was followed.[23,34] The reaction was also performed with empty beads, but otherwise under the same conditions as above. The results obtained are shown in Figure 7A. In the figure, the time course of the OD_{600} value observed with single empty beads shows the onset of increase in the value at about 2 min. With the beads entrapped with BCALs, the OD_{600} values for the initial 2 min are slightly larger than the reaction with empty beads, although the data scattered. The rate of increase in the OD_{600} value after the

https://dx.doi.org/10.1021/acsomega.0c06299
ACS Omega 2021, 6, 6368−6378

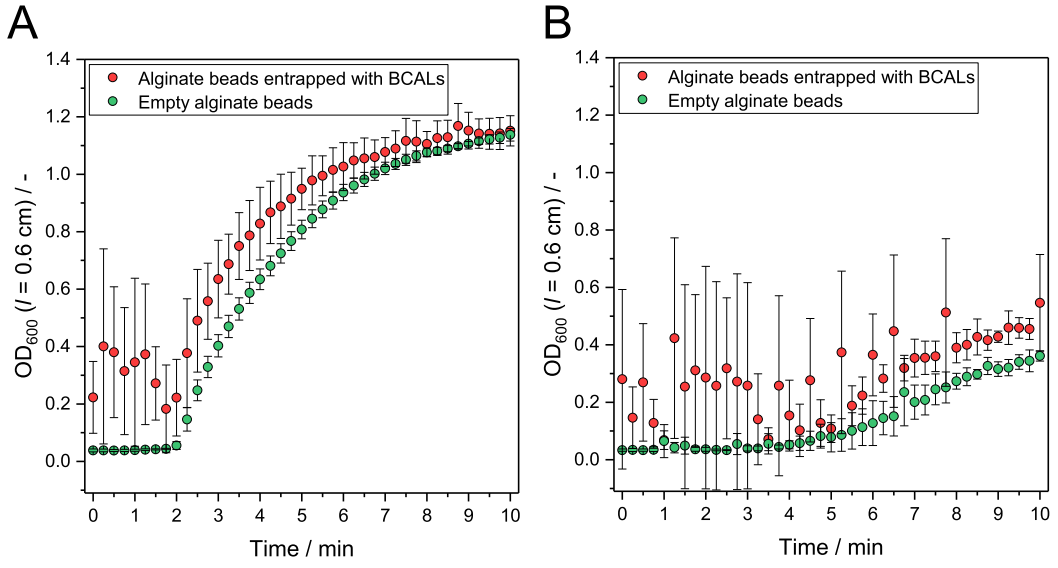

Figure 7. (A) Time courses of the turbidity (OD_{600}) of the mixtures, which were prepared by mixing 1.4 M Tris (43.3 μL), 200 mM $CaCl_2$ (46 μL), an alginate bead, and a CO_2-saturated water solution (110.7 μL) in microplate wells. The concentrations of Tris and $CaCl_2$ in the mixtures were 0.3 M and 46 mM, respectively. The total volume of the bulk solution was 200 μL. The results were obtained with empty beads (green circles) or the beads entrapped with BCALs (red circles). (B) Time courses of the OD_{600} values in the reaction mixture being prepared as described above except that the two-times lower initial concentration of CO_2 was employed. All reactions were performed in microplate wells. For each type of bead, three freshly prepared beads were used in three parallel reactions. In a well-contained with a bead, a Tris solution was first mixed with a $CaCl_2$ solution and then a CO_2-containing water solution was added to induce the formation of calcium carbonate. All reactions were performed at about 17 °C without mixing. The data represent mean value ± standard deviation (n = 3).

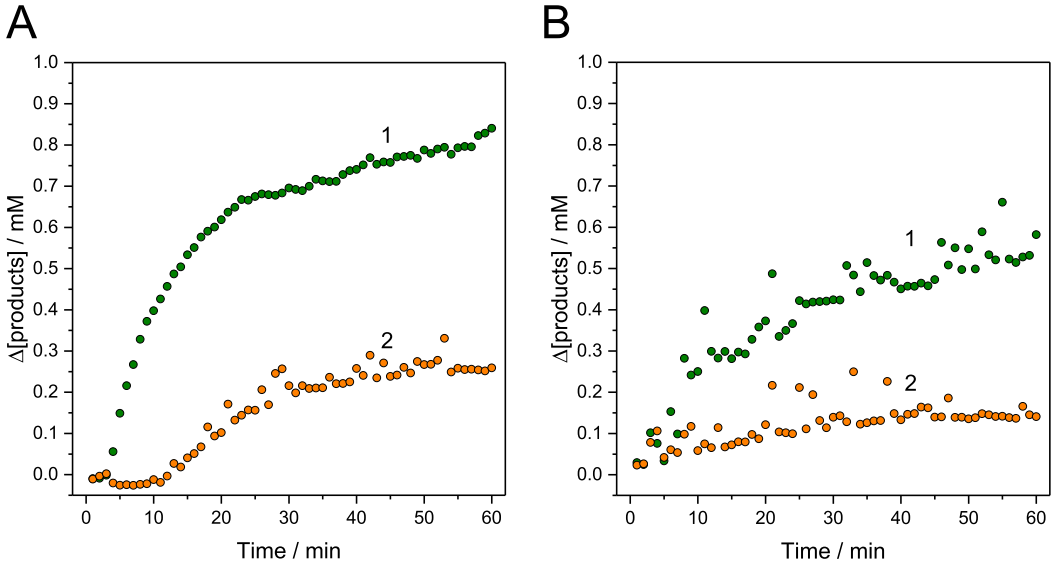

Figure 8. Time courses of the concentrations of catalytically produced products (Δ[products]) in the flow-through reactor confined with the alginate beads. A TB2 solution (pH = 7.5) containing 1.0 mM *p*-NA was passed through the reactor at a constant flow rate of 68 μL/min (A) or 137 μL/min (B). The mean residence time was 8.5 min (A) or 4.3 min (B). The beads confined in the reactor were entrapped with BCALs (curves 1) or free BCA (curves 2). The reaction mixtures were collected every 1 min at the outlet of the reactor and analyzed in terms of the absorbance at 405 nm (A_{405}). The concentration of *p*-nitrophenolate was calculated to be ε_{405} = 10510 $M^{-1}\cdot cm^{-1}$. The total concentration of products ([products] = [*p*-nitrophenolate] + [*p*-nitrophenol]) was then calculated with a pK_a value of 7.14 between the products.[47] To calculate Δ[products] in each figure, the A_{405} values obtained with empty beads were subtracted from the values obtained with the beads entrapped with BCALs or free BCA. For the time courses of the A_{405} values obtained with the beads entrapped with BCALs or free BCA, or empty beads, see Figure S11.

reaction time of 2 min being observed with the beads entrapped with BCALs is slightly larger than the rate with the empty beads. Nevertheless, the catalytic activity of BCALs being entrapped in alginate beads was not clear when one applied the beads to promote the formation of calcium carbonate with water-dissolved CO_2 as one of the feed materials. A similar result was obtained when the reaction was performed at two-times lower initial concentration of CO_2 (Figure 7B). On the other hand, unentrapped BCALs clearly promoted the formation of calcium carbonate particles through catalyzing the hydration of CO_2, see Figure S9. The alginate molecules were reported to be interactive with calcium

https://dx.doi.org/10.1021/acsomega.0c06299
ACS Omega 2021, 6, 6368−6378

carbonate.[35−37] The above results suggest that the interactions among anionic lipid bilayers, alginate matrices, and/or calcium ions being present in both the bulk solution and the beads can partly hinder the catalytic activity of the BCALs in the beads. The enzyme-conjugated lipid bilayers being densely present in the beads may potentially affect the physicochemical properties at the surface region of the beads in the presence of high concentrations of calcium ions and CO_2 in the bulk solution. The alginate beads entrapped with free BCA exhibited the catalytic activity in the CO_2 hydration (Figure S10), although the contribution of free BCA leached from the beads into the bulk solution needs to be considered.

Continuous-Flow Hydrolysis of *p*-NA Catalyzed by Alginate Beads Entrapped with BCALs. Immobilized biocatalysts can give opportunities to continuously operate reactors for various purposes.[38−43] Support materials for enzyme immobilization can provide spatially or interfacially controlled reaction environments being potentially advantageous for multiple enzyme-catalyzed or bioelectrochemical reactions.[44−46] The alginate beads entrapped with BCALs were confined in a flow-through column and a TB2 solution containing 1.0 mM *p*-NA was passed continuously through the reactor. The absorbance at 405 nm was measured with respect to the fractions collected at the outlet of the reactor. The results obtained at a flow rate of 68 μL/min corresponding to the mean residence time τ of 8.5 min are shown in Figure 8A. For the reaction catalyzed by the beads entrapped with BCALs (curve 1), the high concentrations of catalytically produced products (Δ[products] = Δ[*p*-nitrophenolate] + Δ[*p*-nitrophenol])[42,43,47] are seen at the reactor outlet for the operation time ranging from 20 to 60 min, see Figure S11 for details including the reactions with empty beads. At an operation time of 60 min, the Δ[products] value reaches 0.84 mM, meaning that 84% of the substrate was catalytically converted into the products by being passed through the reactor. For the flow reaction with the alginate beads entrapped with free BCA (curve 2 in Figure 8A), the concentrations of products are significantly lower than these obtained with the beads entrapped with BCALs in consistent with the difference in the amounts of enzyme entrapped in each bead. At a higher flow rate of 137 μL/min (τ = 4.3 min) (Figure 8B), the concentrations of catalytically produced products with the beads entrapped with BCALs decrease as compared to the reaction at τ = 8.5 min (Figure 8A). A similar trend is also seen with respect to the reaction catalyzed by the beads entrapped with free BCA. The above results clearly demonstrate that the alginate beads entrapped with BCALs function as the catalyst for the continuous-flow reactions in which the conversion at the reactor outlet is controllable on the basis of the flow rate.

CONCLUSIONS

The present work reports an approach to efficiently and stably entrap BCALs in calcium alginate hydrogel beads. The BCALs, which possess a much larger hydrodynamic diameter than free BCA molecules, could be entrapped in alginate beads with a high entrapment efficiency of 98.7% without any additional treatment of the beads such as surface coating with cationic polymers. The alginate beads entrapped with BCALs possessed an average diameter of 2.7 mm, therefore, the beads were easy to handle. On the other hand, the entrapment efficiency of free BCA was 27.7%, clearly meaning that leaching of the free enzyme molecules from the alginate beads occurred. The integrity of intact lipid membranes was not significantly affected by the entrapment of liposomes in the alginate beads, as revealed on the basis of the observation that the 5(6)-carboxyfluorescein molecules were stably encapsulated in the enzyme-free liposomes during the series of entrapment processes. The catalytic performance of the alginate beads entrapped with BCALs was examined using the microplate wells as small-volume reaction vessels in which single beads were used as catalysts. The beads showed the esterase activity toward 1.0 mM *p*-NA, although the mass transfer effects caused the decrease in the rate of reactions compared to the case of unentrapped BCALs-catalyzed reactions. The alginate beads entrapped with BCALs showed stable catalytic activity when the beads were used for repeated bath reactions, whereas the beads entrapped with free BCA became almost inactive after the first reaction-washing cycle probably because of significant leaching of the enzyme from the beads. The alginate beads entrapped with BCALs could not efficiently catalyze the hydration of CO_2 to induce the formation of calcium carbonate. The beads entrapped with BCALs were confined in the reactor column and applied to the continuous-flow hydrolysis of 1.0 mM *p*-NA for 1 h at the mean residence time τ of 8.5 or 4.3 min. The concentrations of hydrolysis products at the reactor outlet were dependent on the flow rate. The fractional conversion of the substrate on the basis of catalytically produced products reached 84% at a flow rate of 68 μL/min corresponding to τ = 8.5 min. Our approach is potentially applicable to efficient and stable entrapment of other enzymes with various molecular sizes in hydrogels. The hydrogel beads entrapped with enzyme-conjugated liposomes may have potential application to multienzyme-catalyzed reactions being examined so far with vesicles[48−50] or various hydrogel systems.[51−53]

ASSOCIATED CONTENT

Supporting Information

The Supporting Information is available free of charge at https://pubs.acs.org/doi/10.1021/acsomega.0c06299.

Preparation of BCALs; effects of preparation conditions on the stability of alginate beads; relationship between esterase activity and concentration of free BCA; preparation of CFLs; photographs of various alginate hydrogel beads; entrapment efficiency of BCALs or free BCA in alginate beads; batch hydrolysis with alginate beads entrapped with free BCA; repeated batch reactions with bead-entrapped enzymes; hydration of CO_2 catalyzed by unentrapped BCALs; hydration of CO_2 with alginate beads entrapped with free BCA; and continuous-flow hydrolysis of *p*-NA (PDF)

AUTHOR INFORMATION

Corresponding Author

Makoto Yoshimoto − *Department of Applied Chemistry, Yamaguchi University, Ube 755-8611, Japan*; orcid.org/0000-0001-7489-229X; Phone: +81-836-85-9271; Email: yosimoto@yamaguchi-u.ac.jp; Fax: +81-836-85-9201

Author

Junshi Moriyama − *Department of Applied Chemistry, Yamaguchi University, Ube 755-8611, Japan*

Complete contact information is available at: https://pubs.acs.org/10.1021/acsomega.0c06299

https://dx.doi.org/10.1021/acsomega.0c06299
ACS Omega 2021, 6, 6368−6378

Author Contributions

This article was written through contributions of J.M. and M.Y.

Notes

The authors declare no competing financial interest.

■ ACKNOWLEDGMENTS

This work was supported by the JSPS KAKENHI grant number JP 20H02543.

■ REFERENCES

(1) Grant, G. T.; Morris, E. R.; Rees, D. A.; Smith, P. J. C.; Thom, D. Biological interactions between polysaccharides and divalent cations: The egg-box model. *FEBS Lett.* **1973**, *32*, 195−198.
(2) Kierstan, M.; Bucke, C. The immobilization of microbial cells, subcellular organelles, and enzymes in calcium alginate gels. *Biotechnol. Bioeng.* **1977**, *19*, 387−397.
(3) Zhu, H.; Srivastava, R.; Brown, J. Q.; McShane, M. J. Combined physical and chemical immobilization of glucose oxidase in alginate microspheres improves stability of encapsulation and activity. *Bioconjugate Chem.* **2005**, *16*, 1451−1458.
(4) Tan, W.-H.; Takeuchi, S. Monodisperse alginate hydrogel microbeads for cell encapsulation. *Adv. Mater.* **2007**, *19*, 2696−2701.
(5) Kupikowska-Stobba, B.; Lewińska, D. Polymer microcapsules and microbeads as cell carriers for *in vivo* biomedical applications. *Biomater. Sci.* **2020**, *8*, 1536−1574.
(6) Kang, S.-M.; Lee, J.-H.; Huh, Y. S.; Takayama, S. Alginate microencapsulation for three-dimensional in vitro cell culture. *ACS Biomater. Sci. Eng.* **2020**, DOI: 10.1021/acsbiomaterials.0c00457.
(7) Li, Y.; Rodrigues, J.; Tomás, H. Injectable and biodegradable hydrogels: gelation, biodegradation and biomedical applications. *Chem. Soc. Rev.* **2012**, *41*, 2193−2221.
(8) Thakar, H.; Sebastian, S. M.; Mandal, S.; Pople, A.; Agarwal, G.; Srivastava, A. Biomolecule-conjugated macroporous hydrogels for biomedical applications. *ACS Biomater. Sci. Eng.* **2019**, *5*, 6320−6341.
(9) Lassouane, F.; Aït-Amar, H.; Amrani, S.; Rodriguez-Couto, S. A promising laccase immobilization approach for Bisphenol A removal from aqueous solutions. *Bioresour. Technol.* **2019**, *271*, 360−367.
(10) Boyaval, P.; Goulet, J. Optimal conditions for production of lactic acid from cheese whey permeate by Ca-alginate-entrapped *Lactobacillus helveticus*. *Enzyme Microb. Technol.* **1988**, *10*, 725−728.
(11) Mallardi, A.; Angarano, V.; Magliulo, M.; Torsi, L.; Palazzo, G. General approach to the immobilization of glycoenzyme chains inside calcium alginate beads for bioassay. *Anal. Chem.* **2015**, *87*, 11337−11344.
(12) Martinsen, A.; SkjÅk-Braek, G.; Smidsrød, O. Alginate as immobilization material: I. Correlation between chemical and physical properties of alginate gel beads. *Biotechnol. Bioeng.* **1989**, *33*, 79−89.
(13) Bajpai, S. K.; Sharma, S. Investigation of swelling/degradation behavior of alginate beads crosslinked with Ca^{2+} and Ba^{2+} ions. *React. Funct. Polym.* **2004**, *59*, 129−140.
(14) Jin, Z.; Harvey, A. M.; Mailloux, S.; Halámek, J.; Bocharova, V.; Twiss, M. R.; Katz, E. Electrochemically stimulated release of lysozyme from an alginate matrix cross-linked with iron cations. *J. Mater. Chem.* **2012**, *22*, 19523−19528.
(15) Simsek-Ege, F. A.; Bond, G. M.; Stringer, J. Matrix molecular weight cut-off for encapsulation of carbonic anhydrase in polyelectrolyte beads. *J. Biomater. Sci. Polym. Ed.* **2002**, *13*, 1175−1187.
(16) Won, K.; Kim, S.; Kim, K.-J.; Park, H. W.; Moon, S.-J. Optimization of lipase entrapment in Ca-alginate gel beads. *Process Biochem.* **2005**, *40*, 2149−2154.
(17) Nguyen, L. T.; Yang, K.-L. Combined cross-linked enzyme aggregates of horseradish peroxidase and glucose oxidase for catalyzing cascade chemical reactions. *Enzyme Microb. Technol.* **2017**, *100*, 52−59.
(18) Nawawi, N. N.; Hashim, Z.; Rahman, R. A.; Murad, A. M. A.; Bakar, F. D. A.; Illias, R. M. Entrapment of porous cross-linked enzyme aggregates of maltogenic amylase from *Bacillus lehensis* G1 into calcium alginate for maltooligosaccharides synthesis. *Int. J. Biol. Macromol.* **2020**, *150*, 80−89.
(19) Takagi, I.; Shimizu, H.; Yotsuyanagi, T. Application of alginate gel as a vehicle for liposomes. I. Factors affecting the loading of drug-containing liposomes and drug release. *Chem. Pharm. Bull.* **1996**, *44*, 1941−1947.
(20) Ullrich, M.; Hanuš, J.; Dohnal, J.; Štěpánek, F. Encapsulation stability and temperature-dependent release kinetics from hydrogel-immobilised liposomes. *J. Colloid Interface Sci.* **2013**, *394*, 380−385.
(21) Sawant, R. R.; Sriraman, S. K.; Navarro, G.; Biswas, S.; Dalvi, R. A.; Torchilin, V. P. Polyethyleneimine-lipid conjugate-based pH-sensitive micellar carrier for gene delivery. *Biomaterials* **2012**, *33*, 3942−3951.
(22) Yoshimoto, M.; Sakamoto, H.; Shirakami, H. Covalent conjugation of tetrameric bovine liver catalase to liposome membranes for stabilization of the enzyme tertiary and quaternary structures. *Colloids Surf., B* **2009**, *69*, 281−287.
(23) Maeshima, K.; Yoshimoto, M. Preparation and characterization of carbonic anhydrase-conjugated liposomes for catalytic synthesis of calcium carbonate particles. *Enzyme Microb. Technol.* **2017**, *105*, 9−17.
(24) Itel, F.; Skovhus Thomsen, J.; Städler, B. Matrix vesicles-containing microreactors as support for bonelike osteoblasts to enhance biomineralization. *ACS Appl. Mater. Interfaces* **2018**, *10*, 30180−30190.
(25) Mirjafari, P.; Asghari, K.; Mahinpey, N. Investigating the application of enzyme carbonic anhydrase for CO_2 sequestration purposes. *Ind. Eng. Chem. Res.* **2007**, *46*, 921−926.
(26) Kim, S.; Joo, K. I.; Jo, B. H.; Cha, H. J. Stability-controllable self-immobilization of carbonic anhydrase fused with a silica-binding tag onto diatom biosilica for enzymatic CO_2 capture and utilization. *ACS Appl. Mater. Interfaces* **2020**, *12*, 27055−27063.
(27) Ren, S.; Jiang, S.; Yan, X.; Chen, R.; Cui, H. Challenges and Opportunities: Porous Supports in Carbonic Anhydrase Immobilization. *J. CO2 Util.* **2020**, *42*, 101305.
(28) Yoshimoto, M.; Walde, P. Immobilized carbonic anhydrase: preparation, characteristics and biotechnological applications. *World J. Microbiol. Biotechnol.* **2018**, *34*, 151.
(29) Lindskog, S. Purification and Properties of bovine erythrocyte carbonic anhydrase. *Biochim. Biophys. Acta* **1960**, *39*, 218−226.
(30) Innocenti, A.; Scozzafava, A.; Parkkila, S.; Puccetti, L.; De Simone, G.; Supuran, C. T. Investigations of the esterase, phosphatase, and sulfatase activities of the cytosolic mammalian carbonic anhydrase isoforms I, II, and XIII with 4-nitrophenyl esters as substrates. *Bioorg. Med. Chem. Lett.* **2008**, *18*, 2267−2271.
(31) Yoshimoto, M.; Tamura, R.; Natsume, T. Liposome clusters with shear stress-induced membrane permeability. *Chem. Phys. Lipids* **2013**, *174*, 8−16.
(32) Gao, J.; Whitesides, G. M. Using protein charge ladders to estimate the effective charges and molecular weights of proteins in solution. *Anal. Chem.* **1997**, *69*, 575−580.
(33) Favre, N.; Christ, M. L.; Pierre, A. C. Biocatalytic capture of CO_2 with carbonic anhydrase and its transformation to solid carbonate. *J. Mol. Catal. B: Enzym.* **2009**, *60*, 163−170.
(34) Yadav, R. R.; Mudliar, S. N.; Shekh, A. Y.; Fulke, A. B.; Devi, S. S.; Krishnamurthi, K.; Juwarkar, A.; Chakrabarti, T. Immobilization of carbonic anhydrase in alginate and its influence on transformation of CO_2 to calcite. *Process Biochem.* **2012**, *47*, 585−590.
(35) Abalymov, A.; Van der Meeren, L.; Saveleva, M.; Prikhozhdenko, E.; Dewettinck, K.; Parakhonskiy, B.; Skirtach, A. G. Cells-grab-on particles: a novel approach to control cell focal adhesion on hybrid thermally annealed hydrogels. *ACS Biomater. Sci. Eng.* **2020**, *6*, 3933−3944.
(36) Xu, N.; Xu, J.; Zheng, X.; Hui, J. Preparation of Injectable Composite Hydrogels by Blending Poloxamers with Calcium Carbonate-Crosslinked Sodium Alginate. *ChemistryOpen* **2020**, *9*, 451−458.

https://dx.doi.org/10.1021/acsomega.0c06299
ACS Omega 2021, 6, 6368−6378

(37) Browning, K. L.; Stocker, I. N.; Gutfreund, P.; Clarke, S. M. The effect of alginate composition on adsorption to calcium carbonate surfaces. *J. Colloid Interface Sci.* **2021**, *581*, 682−689.
(38) Liu, M.; Yong, Q.; Lian, Z.; Huang, C.; Yu, S. Continuous bioconversion of oleuropein from olive leaf extract to produce the bioactive product hydroxytyrosol using carrier-immobilized enzyme. *Appl. Biochem. Biotechnol.* **2020**, *190*, 148−165.
(39) Tepe, O.; Dursun, A. Y. Combined effects of external mass transfer and biodegradation rates on removal of phenol by immobilized *Ralstonia eutropha* in a packed bed reactor. *J. Hazard. Mater.* **2008**, *151*, 9−16.
(40) De Santis, P.; Meyer, L.-E.; Kara, S. The rise of continuous flow biocatalysis—fundamentals, very recent developments and future perspectives. *React. Chem. Eng.* **2020**, *5*, 2155−2184.
(41) Zhu, Y.; Li, W.; Sun, G.; Tang, Q.; Bian, H. Enzymatic properties of immobilized carbonic anhydrase and the biocatalyst for promoting CO_2 capture in vertical reactor. *Int. J. Greenhouse Gas Control* **2016**, *49*, 290−296.
(42) Yoshimoto, M.; Schweizer, T.; Rathlef, M.; Pleij, T.; Walde, P. Immobilization of carbonic anhydrase in glass micropipettes and glass fiber filters for flow-through reactor applications. *ACS Omega* **2018**, *3*, 10391−10405.
(43) Ghéczy, N.; Sasaki, K.; Yoshimoto, M.; Pour-Esmaeil, S.; Kröger, M.; Stano, P.; Walde, P. A two-enzyme cascade reaction consisting of two reaction pathways. Studies in bulk solution for understanding the performance of a flow-through device with immobilised enzymes. *RSC Adv.* **2020**, *10*, 18655−18676.
(44) Chen, H.; Simoska, O.; Lim, K.; Grattieri, M.; Yuan, M.; Dong, F.; Lee, Y. S.; Beaver, K.; Weliwatte, S.; Gaffney, E. M.; Minteer, S. D. Fundamentals, applications, and future directions of bioelectrocatalysis. *Chem. Rev.* **2020**, *120*, 12903−12993.
(45) Dubey, N. C.; Tripathi, B. P. Nature inspired multienzyme immobilization: strategies and concepts. *ACS Appl. Bio Mater.* **2021**, *4*, 1077−1114.
(46) Metzger, K. E.; Moyer, M. M.; Trewyn, B. G. Tandem catalytic systems integrating biocatalysts and inorganic catalysts using functionalized porous materials. *ACS Catal.* **2021**, *11*, 110−122.
(47) Grzyska, P. K.; Czyryca, P. G.; Purcell, J.; Hengge, A. C. Transition state differences in hydrolysis reactions of alkyl versus aryl phosphate monoester monoanions. *J. Am. Chem. Soc.* **2003**, *125*, 13106−13111.
(48) Elani, Y.; Law, R. V.; Ces, O. Vesicle-based artificial cells as chemical microreactors with spatially segregated reaction pathways. *Nat. Commun.* **2014**, *5*, 5305.
(49) Fujiwara, K.; Adachi, T.; Doi, N. Artificial cell fermentation as a platform for highly efficient cascade conversion. *ACS Synth. Biol.* **2018**, *7*, 363−370.
(50) Nagatomo, N.; Yoshimoto, M. High permeability of polyunsaturated lipid bilayers as applied to attoliter enzyme reactors. *ACS Appl. Bio Mater.* **2019**, *2*, 2453−2463.
(51) Kim, S.; Kwon, K.; Cha, J.; Yoo, S.; Han, M. S.; Tae, G.; Kwon, I. Pluronic-based nanocarrier platform encapsulating two enzymes for cascade reactions. *ACS Appl. Bio Mater.* **2020**, *3*, 5126−5135.
(52) Tan, H.; Guo, S.; Dinh, N.-D.; Luo, R.; Jin, L.; Chen, C.-H. Heterogeneous multi-compartmental hydrogel particles as synthetic cells for incompatible tandem reactions. *Nat. Commun.* **2017**, *8*, 663.
(53) Liang, H.; Jiang, S.; Yuan, Q.; Li, G.; Wang, F.; Zhang, Z.; Liu, J. Co-immobilization of multiple enzymes by metal coordinated nucleotide hydrogel nanofibers: improved stability and an enzyme cascade for glucose detection. *Nanoscale* **2016**, *8*, 6071−6078.

https://dx.doi.org/10.1021/acsomega.0c06299
ACS Omega 2021, 6, 6368−6378